THE JOURNAL OF PHYSICAL CHEMISTRY A

ARTICLE

pubs.acs.org/JPCA

Bond Energies, Reaction Volumes, and Kinetics for σ- and π-Complexes of $Mo(CO)_5L$

Shannon M. Gittermann, Roger G. Letterman, Tianjie Jiao, Ging-Long Leu, Nathan J. DeYonker, Charles Edwin Webster, and Theodore J. Burkey*

Department of Chemistry, The University of Memphis, Memphis, Tennessee 38152-3550, United States

Supporting Information

ABSTRACT: The photosubstitution reactions of molybdenum hexacarbonyl with σ and π donor ligands were investigated using photoacoustic calorimetry and computational methods in a series of linear alkane solvents (pentane, hexane, heptane, octane, decane, and dodecane). The results show that reaction volumes make a significant contribution to the photoacoustic signal and must be considered during thermodynamic calculations based on photoacoustic measurements. The enthalpies of CO substitution by an alkane solvent and subsequent substitution by each Lewis base were determined. Corresponding Mo−L bond energies (kcal mol^{-1}) were calculated: L = linear alkanes (13), triethylsilane (26), 1-hexyne (27), 1-hexene (27), and benzene (17). The relative energies are in agreement with computational results. The experimental reaction volume for CO substitution by alkane was positive (15 mL mol^{-1}) and negative or close to zero for alkane substitution by a Lewis base (for example, −11 mL mol^{-1} for triethylsilane and 3.6 mL mol^{-1} for benzene). The errors in the experimental and computational reaction volumes are large and often comparable to the reaction volumes. An improved calibration of the methods as well as a better understanding of the underlying physics involved is needed. For the Lewis bases reported in this study, the second-order rate constants for the displacement of a coordinated alkane are less than diffusion control (5×10^6−4×10^7 M^{-1} s^{-1}) and decrease monotonically with the alkane chain length. The rate constants correlate better with steric effects than with bond energies. An interchange mechanism is consistent with the results.

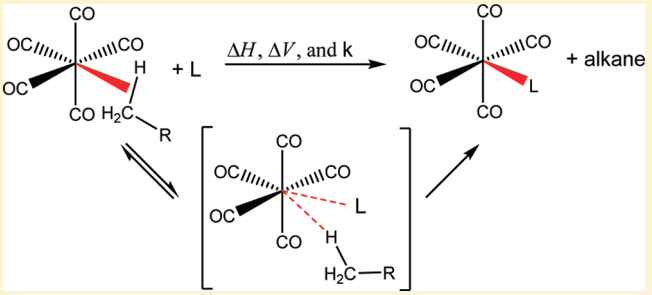

INTRODUCTION

Bond energies are a valuable tool for understanding which bonds are broken or formed when preparing organometallic compounds and molecular devices. In particular, we are interested in preparing photochromic materials based on organometallic complexes that can undergo a light-driven linkage isomerization (Scheme 1).[1] To avoid fatigue, low quantum yields and, ultimately, the loss of the photochromic response, it is imperative that irradiation selectively cleaves only the M−X or the M−Y bond. In many complexes, there is a general trend that near-UV radiation breaks the weakest bond. Thus, it is useful to know the bond energies when designing photochromic compounds.[2] Unfortunately, the magnitudes of many metal−ligand bond energies are not well established.[3] Many bond energies determined in solution are based on activation enthalpies of ligand dissociation; however, ligand dissociation in solution often involves the solvent in the transition state and the extent of solvation may be unclear.[4] In general, accurate bond energies, either experimental or computational, are needed to understand and predict the bond energy difference required for selective bond cleavage.

We have been investigating photoacoustic calorimetry (PAC) as a tool for determining absolute and relative metal−ligand bond energies. In particular, it has been determined that neglecting reaction volumes can lead to erroneous PAC results.[5] Unfortunately, a 6-fold increase in the number of PAC experiments is required to determine the contribution of reaction volumes, and we have been exploring if this experimental burden can be reduced by independently calculating the reaction volumes using computational methods.

In this study, we report the ligand photosubstitution of molybdenum hexacarbonyl with π- or σ-donor ligands in an effort to examine how these ligand structures affect PAC measurements. Ultrafast time-resolved studies of molybdenum hexacarbonyl in an alkane solvent show that irradiation leads to dissociation of CO followed by solvent coordination (<1 ps) in

Scheme 1

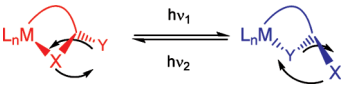

Received: April 27, 2011
Revised: June 23, 2011
Published: July 22, 2011

Scheme 2

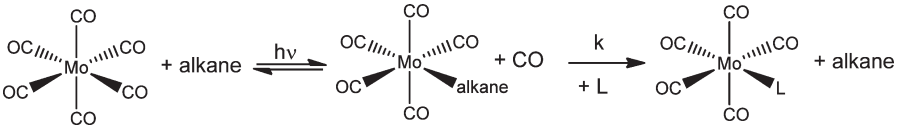

competition with cage CO recombination (Scheme 2, first step). Ultrafast solvent coordination can occur even for solvents as weakly basic as alkanes.[6] Thermal relaxation of the metal-alkane complex is complete in a few hundred picoseconds,[6,7] and depending on the concentration of the Lewis base, *L*, the second step is typically on the microsecond time scale[4,8] where the observed rate constant (k_{obs}) is directly related to the microscopic rate constant k (eq 1). Following a laser pulse, PAC can resolve the acoustic waves of the faster processes of the first step from those of the second step. The results are used to determine the enthalpy of each step and the rate constant for the second step.

$$\frac{d[Mo(CO)_5L]}{dt} = k_{obs}[Mo(CO)_5\ alkane] = k[L][Mo(CO)_5\ alkane] \quad (1)$$

Because the differences in the energies of bonds that are broken and formed determine the enthalpy of each step, several bond energies can be calculated from the enthalpies of a single reference bond energy (in this case from Mo−CO). A number of studies have presented gas-phase (experimental[9] and computational[10]) and solution-phase (experimental[4,11]) strengths of metal−alkane bonds. Previously, we reported results for Mo−alkane bond energies as well as those for ligands that bond via lone pairs.[5,12] Currently, we present PAC results for π- or σ-complexes with 1-hexyne, 1-hexene, benzene, triethylsilane, and a series of linear alkanes (*n*-pentane, *n*-hexane, *n*-heptane, *n*-octane, *n*-decane, and *n*-dodecane). Theoretical molybdenum-ligand bond energies were computed for the same ligands except the alkane series was methane, ethane, *n*-propane, *n*-butane, *n*-pentane, *n*-hexane, and *n*-heptane.

EXPERIMENTAL SECTION

Materials. Unless otherwise noted, materials were purchased from Sigma Aldrich. Molybdenum hexacarbonyl (Strem) and ferrocene (Ethyl) were sublimed before use. Anhydrous solvents were purchased with the exception of hexane, which was distilled from NaK under argon. Decane, octane, and dodecane were recycled by washing with sulfuric acid and water, drying with magnesium sulfate, passing through silica gel, 10% silver nitrate on silica, and refluxing under argon with sodium. All solvents were kept under argon or nitrogen. Ligands were checked for impurities by GC/MS and NMR spectroscopy. The optical purity of solvents was determined by UV spectroscopy, and ligand purity was confirmed by NMR spectroscopy or mass spectrometry.

Equipment. Optical absorbances were determined with a Gilford 240 spectrophotometer. NMR and mass spectra were obtained with a JEOL 270 MHz NMR spectrometer and an HP G1800A GCD system, respectively. The photoacoustic calorimeter, described previously, has a PTI GL3300 (900 ps fwhm) or Laser Science VSL-337 (5 ns fwhm) nitrogen laser (337.1 nm) and Panametrics A103S transducers (see Supporting Information for a diagram of PAC). The beam was focused to 1 mm with 20 μJ/pulses or less.

Sample Preparation. All $Mo(CO)_6$ solutions were prepared under nitrogen. Ferrocene and molybdenum hexacarbonyl concentrations were adjusted so that A_{337} (absorbance at 337 nm) ≈ 0.11. Ferrocene was used as a reference because it quantitatively converts the photon energy to heat.[13] In a typical experiment, a stock solution was prepared in a glovebox with 12 mg (0.077 mmol) of molybdenum hexacarbonyl dissolved in 50 mL of decane (A_{337} = 0.436). A dilute stock solution (200 mL, A_{337} = 0.112) was prepared from 46 mL of the molybdenum hexacarbonyl stock solution. Four of the eight solutions for PAC measurements were prepared by diluting 50, 125, 200, and 275 μL of benzene to 25 mL with the dilute molybdenum hexacarbonyl stock solution. The other four solutions were similarly prepared with ferrocene outside the glovebox.

PAC Data Collection. PAC theory and experiments have been described previously.[5,14] All PAC solutions were purged with helium prior to irradiation. To minimize the effect of instrument drift, measurements of ferrocene and molybdenum hexacarbonyl solutions were alternately obtained for each concentration of Lewis base in each solvent. An average of six measurements of molybdenum hexacarbonyl solutions (0.03 mL s^{-1} flow rate) and eight for ferrocene solutions (static) were obtained using a quartz flow cell (0.3 cm wide and 1 cm path length). This procedure was repeated for each ligand concentration in random order.

Following absorption of the laser pulse, a volume change creates an ultrasonic sound wave that is detected with an ultrasonic pressure transducer. The volume change has two components: thermal expansion of solution from heat liberated by light initiated processes ($\Delta V_{thermal}$) and differences in volumes of reactants and intermediates or products (reaction volume, ΔV_{rxn}, eq 2). The sample transducer signal amplitudes were corrected for variations in laser pulse energy and solution absorbance and then

$$\phi = \frac{\Delta V_{thermal} + \Delta V_{rxn}}{\Delta V_{ref}} \quad (2)$$

normalized relative to the reference (ferrocene) signal (ΔV_{ref}). The acoustic signals from the transducer were collected using AQPAC6 (in house program), and the waveforms were deconvoluted using Quantum Northwest Sound Analysis[15,16] yielding a simulated sample signal with an amplitude as a fraction (ϕ) of the reference signal (ferrocene) where all light energy is deposited as heat (Φ = 1.00).[17] The amplitude and phase of the experimental signal typically depends on fast (ϕ_1, τ_1 < 100 ns) and slow components (ϕ_2, τ = 100 ns to 5 μs), where the time resolution is determined by the transducer response time. Measurements of acoustic signals were averaged from sixteen pulses that did not vary more than 0.5 μJ. The heat deposition depends on the energy of the photons and the enthalpy of reaction; therefore, the fractional amplitude (ϕ_1) of the signal for processes much faster than the response time of the transducer depends on the energy of the photon ($h\nu$), the quantum yield (Φ),[18,19] and the thermoelastic properties of the solvent ($\chi = MW\beta/C_p\rho$, where MW = molecular weight, β = coefficient of thermal expansion, C_p = molar heat capacity, ρ = density, eq 3). Rearrangement of eq 3 yields eq 4, and

dx.doi.org/10.1021/jp203915q |J. Phys. Chem. A 2011, 115, 9004–9013

the slope and intercept of a plot of $h\nu\chi(1 - \phi_1)/\Phi$ versus χ provides ΔH_1 and ΔV_1, respectively. The fractional amplitude for the slow component of the signal likewise can be expressed (eqs 5 and 6). A series of linear alkanes were used to vary the solvent thermoelastic properties, and the calculations assume that the metal−solvent bond energy does not vary significantly for the different alkane chain lengths.[12,19]

$$\phi_1 = \frac{h\nu\chi - \Phi\Delta H_1\chi + \Phi\Delta V_1}{h\nu\chi} \quad (3)$$

$$\frac{h\nu\chi(1-\phi_1)}{\Phi} = \Delta H_1\chi - \Delta V_1 \quad (4)$$

$$\phi_2 = -\frac{\Phi(\Delta H_2\chi - \Delta V_2)}{h\nu\chi} \quad (5)$$

$$\frac{-h\nu\chi\phi_2}{\Phi} = \Delta H_2\chi - \Delta V_2 \quad (6)$$

Computational Methods. Theoretical calculations have been carried out using the Gaussian 09[20] implementation of BVP86 [the Becke exchange functional (B)[21] and the Perdew correlation functional (VP86)[22]] density functional theory,[23] using the default pruned fine grids for energies (75, 302), default pruned coarse grids for gradients and Hessians (35, 110; neither grid is pruned for transition metals), and default SCF convergence for geometry optimizations (10^{-8}). BS1: The basis sets for cobalt, chromium, iron, ruthenium, zirconium, nickel, copper, palladium, molybdenum, osmium, and tungsten were the Hay and Wadt basis sets and effective core potential (ECP) combinations (LANL2DZ)[24] as modified by Couty and Hall, where the two outermost p functions have been replaced by a split of the optimized 4p, 5p, or 6p functions.[25] The 6-31G(d′)[26,27] basis sets were used for all other atoms. The density fitting approximation[28] for the fitting of the Coulomb potential was used for all BVP86 calculations; auxiliary density-fitting basis functions were generated automatically (by the procedure implemented in Gaussian 09) for the specified AO basis set. Spherical harmonic d functions were used throughout; that is, there are five angular basis functions per d function. All structures were fully optimized, and analytical frequency calculations were performed on all structures to ensure the stationary point is a zero-order saddle point (a local minimum).

The computational molar volumes were determined similar to that described previously.[29,30] The molecular surfaces were computed using the BVP86/BS1 geometries (optimized with Gaussian 09) with the Gaussian 03[31] implementation of geometria polihedro (GePol) algorithm[32−34] via the SCRF keyword [SCRF(PCM,Read)].[35] In the original paper, the Bondi radii[36] (RADII=BONDI) were used. The current study utilized Pauling radii (RADII=PAULING).

RESULTS

Following the 337 nm irradiation of ferrocene and 1-hexyne in octane, a damped sine wave signal was detected from the ultrasonic transducer (Figure 1, reference waveform). For the irradiation of molybdenum hexacarbonyl and 1-hexyne, the amplitude of the signal is smaller (Figure 1, sample waveform) and decreases further with decreasing 1-hexyne concentration as the phase shifts to longer times. Deconvolution of the sample

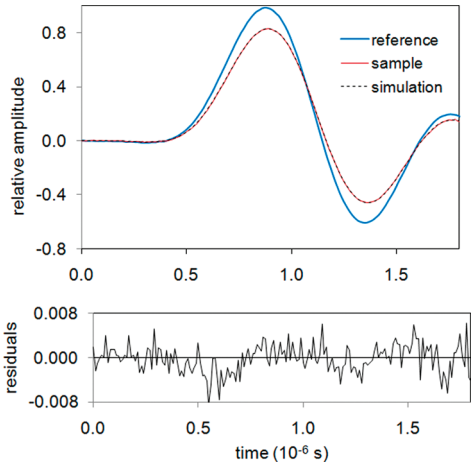

Figure 1. Top: Experimental and simulated PAC signals for irradiation of 5.4 mM ferrocene (reference) or 0.21 mM $Mo(CO)_6$ (sample) with 70 mM 1-hexyne in octane. The parameters for the simulated waveform are $\phi_1 = 0.785$, $\phi_2 = 0.140$, and $\tau = 0.44$ μs. Bottom: residual difference between sample and simulated waveforms, $\chi^2 = 6 \times 10^{-9}$.

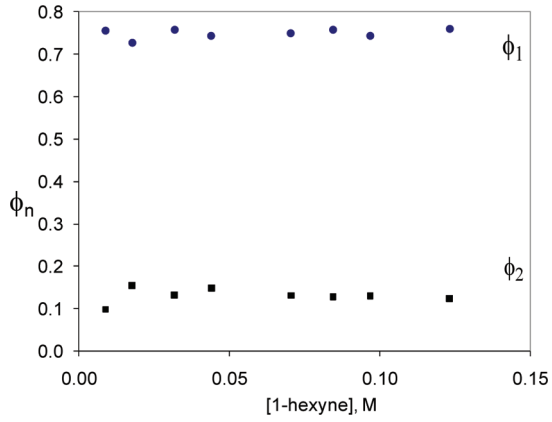

Figure 2. Fractional acoustic amplitudes for photolysis of 0.21 mM $Mo(CO)_6$ with various concentrations of 1-hexyne in octane: ϕ_1 is the amplitude of the signal for processes much faster than the transducer response time, and ϕ_2 is the amplitude of the signal for processes on the same time scale of the transducer response time.

waveform with the reference waveform resolves the fractional signal amplitudes ϕ_1 (generated by processes much faster than the transducer response time) and ϕ_2 (generated by processes on the same time scale as the transducer response time) and provides the lifetime (τ) for the slower signal corresponding to ϕ_2. The amplitudes and lifetimes were used to generate simulated waveforms (Figure 1, top) to determine the goodness of fit from residual differences (Figure 1, bottom). The amplitude ϕ_1 is independent of the concentration (Figure 2) and structure of the Lewis base (Figure 2, Table 1).[37] Likewise, the amplitude ϕ_2 is also independent of the concentration of Lewis base but only over a certain concentration range that is determined by the rate of solvent displacement by the Lewis base (Figure 2);[38] however, the amplitude does depend on the Lewis base structure (Table 1).[39,40]

When molybdenum hexacarbonyl and 1-hexyne were irradiated in a series of linear alkanes, a linear relationship was observed when the response was plotted as a function of χ (eq 3),

Table 1. Summary of ϕ_1, ϕ_2, ΔH_1, ΔH_2, and BE (Bond Energy) Obtained for the Ligand Substitution of $Mo(CO)_6$ in Linear Alkane Solvents[a]

ligand	ϕ_{1H}[b]	ϕ_{2H}[b]	ΔH_1[c]	ΔH_{1H}[b]	ΔH_2[c]	ΔH_{2H}[b]	BE[d]
			kcal mol^{-1}				
benzene	0.765 (29)	0.053 (8)	29.2 (25)	22.1	−4.0 (15)	−5.0	16.5
triethylsilane	0.738 (3)	0.098 (9)	28.9 (15)	24.7	−13.2 (14)	−9.2	25.7
THF[e]	0.751 (11)	0.134 (14)	29.7(17)	23.5	−13.8 (14)	−12.6	26.3
1-hexyne	0.772 (23)	0.147 (10)	26.4 (23)	21.5	−14.0 (17)	−13.9	26.5
1-hexene	0.768 (13)	0.117 (14)	26.3 (30)	21.9	−14.4 (31)	−11.0	26.9
THT[f]	0.747 (13)	0.213 (14)	27.2 (19)	23.8	−23.6 (21)	−20.1	36.1

[a] Values in parentheses are the errors in the last digit(s). [b] Determination in heptane assuming $\Delta V_1 = \Delta V_2 = 0$. [c] Multisolvent determination like that shown in Figure 3. [d] The relative errors for BE (bond energy) are the same as the errors for ΔH_2: BE(M-L) = BE(M-CO) − ΔH_{1avg} − ΔH_2. [e] Tetrahydrofuran, ref 19. [f] Tetrahydrothiophene, ref 12.

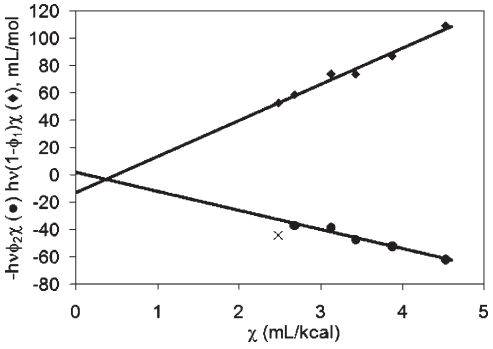

Figure 3. Solvent dependence of acoustic signal following irradiation of $Mo(CO)_6$ with 1-hexyne in linear alkanes.[41]

Table 2. Summary of ΔV_1 and ΔV_2 Obtained by PAC for the Ligand Substitution on $Mo(CO)_6$

ligand	ΔV_1	ΔV_2
	mL mol^{-1}	
1-hexene	10.8 (99)	−9.0 (106)
1-hexyne	12.3 (66)	−2.0 (59)
benzene	19.8 (81)	3.6 (54)
triethylsilane	15.4 (38)	−11.4 (49)
THF	18 (6)	−0.6 (49)
THT	13 (6)	−16 (8)

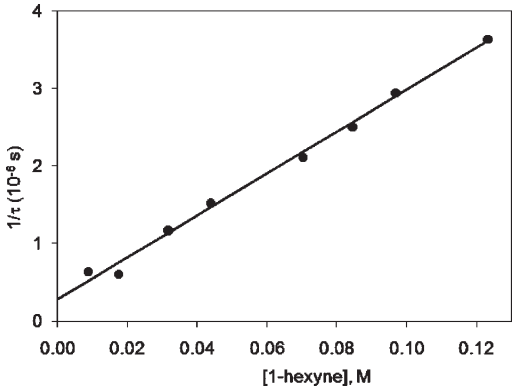

Figure 4. A plot of $1/\tau$ versus [1-hexyne] in octane, slope = 2.7×10^7 M^{-1} s^{-1}.

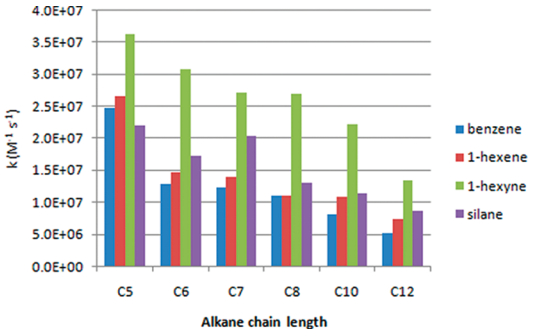

Figure 5. Dependence of the second-order rate constant on *n*-alkane solvent chain length and Lewis base structure.

where the enthalpy and reaction volume are the slope and intercept, respectively (Figure 3). The enthalpies and reaction volumes for different Lewis bases are reported in Tables 1 and 2. The ΔH_1 values are endothermic and the same within experimental error with an average of 28.0 ± 1.5 kcal mol^{-1}. The ΔH_2 values are different for each Lewis base and exothermic. The ΔV_1 values are all positive and have the same value within experimental error with an average of 14.9 ± 3.5 mL mol^{-1}. The ΔV_2 values are all within experimental error of zero or negative depending on the Lewis base. The lifetime τ of the heat decay of ϕ_2, which is assigned to the displacement of solvent by 1-hexyne, varies with 1-hexyne concentration, and a plot of the observed rate constant ($k_{obs} = 1/\tau$) versus the 1-hexyne concentration is linear (Figure 4). A second-order rate constant was obtained from the slope of the plot (Figure 4), and for each Lewis base, the rate constant typically decreased as the alkane chain increased (Figure 5). For a specific solvent, the rate constants were normally in the order 1-hexyne > triethylsilane > 1-hexene > benzene (Table 3).

Computational Results. A total of 40 organometallic complexes (charged and neutral species) with known experimental molar volumes were used as a test set and their structures were optimized using BVP86/BS1. Molecular volumes were computed with GePol and converted to computed molar volumes. The computed molar volume of each species without counterions is shown in Table 4 along with the experimental molar volume with counterions. A plot of the data from Table 4 is shown in Figure 6. A zero intercept is used because a molecule with zero volume would

dx.doi.org/10.1021/jp203915q |J. Phys. Chem. A 2011, 115, 9004–9013

Table 3. Second-Order Rate Constants for Reaction of Lewis Bases with $Mo(CO)_5$(heptane)

L	$k \times 10^{-7}$ M^{-1} s^{-1}
benzene	1.24 (0.4)
1-hexene	1.41 (0.8)
triethylsilane	2.03 (0.2)
1-hexyne	2.70 (0.3)
THF[19]	17 (1)
THT[12]	26 (1)

Table 4. Experimental (Expt) and Computed (Comp) Molar Volumes[a] for Selected Transition Metal Complexes

molar volume (mL mol^{-1})					
neutral compounds[b,c]			charged species[b,c]		
	expt	comp		expt	comp
$Fe(Cp)_2$	141.9	77.0	$[Fe(Cp)_2]^+$	102.2	77.5
$Ru(Cp)_2$	134.8	78.8	$[Co(NH_3)]_6^{3+}$	130.8	81.9
$Os(Cp)_2$	118.2	79.2	$[Fe(CN)_4(C_6H_6N_2)]^{2-}$	116	107.1
$Fe(MeCp)_2$	180.6	96.2	$[Co(en)_3]^{3+}$	190	121.5
$Co(acac)_3$	256.6	158.8	$[Cr(en)_3]^{3+}$	200.6	123.3
$Cr(acac)_3$	257.4	159.3	$[Ni(en)_3]^{2+}$	206.7	123.8
$Fe(Cp^*)_2$	318.7	173.3	$[Co(EDTA)]^{2-}$	166	130.5
$Os(Cp^*)_2$	296.2	175.4	$[Cu(EDTA)]^{2-}$	168	130.7
$Co(dmg)_3(BF)_2$	295.3	176.8	$[Ni(EDTA)]^{2-}$	163.3	130.9
$Fe(bpy)_2(CN)_2$	351.9	181.2	$[Pd(et)_4(dien)(N_3)]^+$	298.1	167.5
$Zr(acac)_4$	347.8	212.5	$[Fe(Cp^*)_2]^+$	308	173.6
$Co(nox)_3(BF)_2$	355.9	217.5	$[Pd(et)_4(dien)(NCS)]^+$	285.9	174.6
$Cr(CNDiip)_6$	1149.5	662.6	$[Co(dmg)_3(BF)_2]^+$	282.5	177.6
$Co(dpg)(BPh)_2$	727.3	424.4	$[Co(nox)_3(BF)_2]^+$	355.5	217.0
$Co(nox)_3(BPh)_2$	462.1	283.8	$[Co(terpy)_2]^{2+}$	418.9	227.7
			$[Fe(bpy)_3]^{2+}$	409	232.6
			$[Co(Dmg)_3(BPh)_2]^+$	417.8	250.2
			$[Fe(phen)]_3^{2+}$	445.1	258.3
			$[Co(phen)]_3^{2+}$	456.3	259.3
			$[Ni(phen)]_3^{2+}$	454.2	261.1
			$[Cu(phen)]_3^{2+}$	456.5	262.2
			$[Co(nox)_3(BPh)_2]^+$	465.8	288.9
			$[Co(Dpg)_3(BPh)_2]^+$	730.3	419.7
			$[Cr(CNDiip)_6]^+$	1178.5	663.8
			$[Cr(CNDiip)_6]^{2+}$	1166.9	664.1

[a] Experimental molar volume data from ref 44. [b] Ligand abbreviations: acac (acetylacetonato), bpy (2,2′−bipyridine), $C_6H_6N_2$ (o-benzoquinone diimine), CNDiip (2,6-diisopropylphenylisocyanide), Cp (cyclopentadienyl), Cp* (pentamethylcyclopentadienyl), dien (diethylenetriamine), dmg (dimethylglyoximato), dpg (diphenylglyoximato), nox (nioximato), en (ethylenediamine), EDTA (ethylenediaminetetraacetato), Et_4dien (tetraethylethylenediamine), MeCp (methylcyclopentadienyl), phen (phenanthroline), terpy (terpyridine). [c] Structures for abbreviated ligands are shown in the Supporting Information.

have a computed zero volume. The linear trend shown is forced through zero with a slope of 1.718 (0.016) and a standard *y*-error of 22.6 mL mol^{-1}.[42] An R^2 value of 0.993 indicates that the molar volumes calculated with the GePol method are well correlated with the experimentally derived volumes. For example, molybdenum pentacarbonyl has a computed molar volume of 63.21 mL mol^{-1},[43] which is multiplied by 1.718 to achieve the empiricized computed molar volume for $Mo(CO)_5$ of 108.60 mL mol^{-1} (as shown in Table 5). It is important to note that the experimental molar volume data for the test set of molecules originated from different solvents, yet the GePol algorithm used a single solvent radius value for determination of the solvent excluding surface.

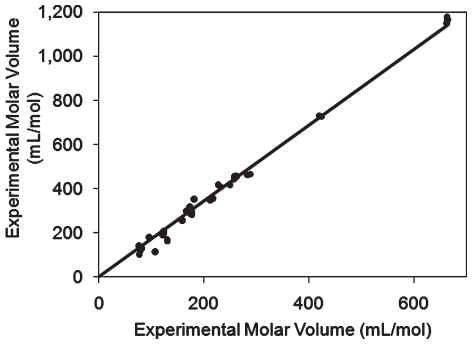

Figure 6. Experimental versus computed molar volumes for charged and neutral species listed in Table 4.

Table 5. Computational Dissociation Enthalpies, Empiricized Computational Molar Volumes, and Empiricized Computational Dissociation Volumes for Linear Alkanes and Molybdenum−Alkane Complexes

compound	computational dissociation enthalpy (kcal mol^{-1})	empiricized computational molar volume (mL mol^{-1})	empiricized computational volume of dissociation (mL mol^{-1})
methane		27.35	
ethane		43.83	
propane		60.45	
butane		76.95	
pentane		93.67	
hexane		110.11	
heptane		126.90	
$Mo(CO)_5$		108.60	
$Mo(CO)_5$(methane)	4.37	135.49	0.46
$Mo(CO)_5$(ethane)	5.12	152.16	0.27
$Mo(CO)_5$(propane)	5.34	168.93	0.12
$Mo(CO)_5$(butane)	5.38	185.47	0.08
$Mo(CO)_5$(pentane)	5.49	202.29	−0.02
$Mo(CO)_5$(hexane)	5.40	218.66	0.05
$Mo(CO)_5$(heptane)	5.15	232.93	2.57

Empiricized computational molar volumes for a series of ligands and molybdenum-ligand complexes are shown in Tables 5−8 along with the computational dissociation enthalpies and empiricized computational dissociation volumes. Computed dissociation enthalpies and dissociation volumes were determined for the dissociation of the ligand from each molybdenum ligand complex listed in Tables 5−8 as products minus reactants. A sample reaction, the dissociation of CO ligand from molybdenum hexacarbonyl, is shown in Scheme 3.

Table 6. Computational Dissociation Enthalpies, Empiricized Computational Molar Volumes, and Empiricized Computational Dissociation Volumes for Linear Alkenes and Molybdenum−Alkene Complexes

compound	computational dissociation enthalpy	empiricized computational molar volume	empiricized computational volume of dissociation
	kcal mol^{-1}	mL mol^{-1}	
ethene		36.34	
1-propene		52.88	
1-butene		69.46	
1-pentene		86.14	
1-hexene		102.63	
$Mo(CO)_5$(ethene)	24.43	144.16	0.78
$Mo(CO)_5$(1-propene)	22.09	160.88	0.60
$Mo(CO)_5$(1-butene)	22.31	178.16	−0.10
$Mo(CO)_5$(1-pentene)	22.41	194.63	0.11
$Mo(CO)_5$(1-hexene)	22.46	211.05	0.18

Table 7. Computational Dissociation Enthalpies, Empiricized Computational Molar Volumes, and Empiricized Computational Dissociation Volumes for Linear Alkynes and Molybdenum−Alkyne Complexes

compound	computational dissociation enthalpy	empiricized computational molar volume	empiricized computational volume of dissociation
	kcal mol^{-1}	mL mol^{-1}	
ethyne		29.06	
1-propyne		45.43	
1-butyne		62.07	
1-pentyne		78.72	
1-hexyne		95.34	
$Mo(CO)_5$(ethyne)	22.98	136.79	0.87
$Mo(CO)_5$(1-propyne)	21.10	153.53	0.50
$Mo(CO)_5$(1-butyne)	21.02	170.13	0.54
$Mo(CO)_5$(1-pentyne)	21.08	186.72	0.60
$Mo(CO)_5$(1-hexyne)	21.18	202.76	1.18

DISCUSSION

Analysis of PAC Signals. The assignments of the PAC signals to specific processes can be determined from known lifetimes of the events following the absorption of light. Following CO dissociation from $Mo(CO)_6$ (100 fs),[45] the addition of alkane solvent to the metal center (<1 ps)[46] competes with CO recombination (300 fs).[47] The metal−solvent σ complex is thermally excited and relaxes (CO stretch) within 200 ps.[7a] These processes cannot be resolved with a 1 MHz transducer and appear as a single fast signal; therefore, the conversion of $Mo(CO)_6$ to $Mo(CO)_5$(alkane) (eq 1, first step) is assigned to this signal. The fact that ϕ_1 (and, therefore, ΔH_1) is independent of the Lewis base structure and concentration indicates that the reaction with the Lewis base does not contribute to the fast component of the PAC signal. For example, no contribution to ϕ_1 is observed until the 1-hexyne concentration is larger than 10 mM (Figure 2). The concentration threshold for contribution to ϕ_1 varies with ligand structure. The contribution detected in ϕ_2 (the slower, phase-shifted component) has a lifetime no greater than 100 ns for concentrations near 0.1 M (Tables 1S−24S in Supporting Information) and indicates that the reactions are slower than diffusion control. Thus, ϕ_2 and ΔH_2 are assigned to the Lewis base displacement of the solvent (eq 1, second step). These results are consistent with lifetimes and rates reported for optical and IR detection of Lewis base addition following irradiation of metal carbonyls in alkane solvents.[48]

The average enthalpy for CO displacement by a linear alkane solvent (ΔH_{1avg}) is endothermic (28.0 ± 1.5 kcal mol^{-1}) and is consistent with substitution of the stronger Mo−CO bond by a weaker M−alkane bond. If it is assumed that ΔV_1 is zero, then χ in eq 4 is eliminated and the enthalpy (ΔH_1) can be calculated for a single solvent. Enthalpies based on this assumption for heptane are reported in Table 1. It is clear that the zero volume assumption leads to an average error of 5 kcal mol^{-1} and an erroneously large calculated value for the metal−alkane bond energy. The large uncertainties in the ΔV values (Table 2) are due to the extrapolation of χ to 0 (e.g., Figure 3) where small errors in the slope can result in large changes in ΔV. In contrast, ΔH is obtained from the slope where the uncertainty is much lower.

Table 8. Computational Dissociation Enthalpies, Empiricized Computational Molar Volumes, and Empiricized Computational Dissociation Volumes for Additional Ligands and Molybdenum−Ligand Complexes

compound	computational dissociation enthalpy	empiricized computational molar volume	empiricized computational volume of dissociation
	kcal mol^{-1}	mL mol^{-1}	
CO		20.75	
THF		74.49	
benzene		76.06	
THT		87.96	
triethylsilane		132.18	
$Mo(CO)_5$(CO)	37.48	127.92	1.43
$Mo(CO)_5$(THF)	19.37	182.57	0.52
$Mo(CO)_5$(benzene)	11.17	184.83	−0.17
$Mo(CO)_5$(THT)	25.28	194.67	1.89
$Mo(CO)_5$(triethylsilane)	15.77	240.00	0.78

In spite of this large uncertainty in reaction volumes, two trends are observed. First, the displacement of CO by alkane has a large positive reaction volume (average ΔV_1 = 14.9 ± 3.5 mL mol^{-1}). The change in volume while breaking the Mo-CO bond is not canceled by the change in volume during the formation of the Mo−alkane bond. Although relative contributions to volume changes are difficult to assign,[49] the formation of a strong bond (like Mo−CO) is expected to reduce the volume since there is a close approach of atoms that form the bond. In contrast, the Mo−alkane bond is weak, the overlap of orbitals is low, and there is not a close approach of atoms that form the bond. Second, the experimental reaction volumes for alkane displacement have a large error but are near zero or negative as the stronger bond

dx.doi.org/10.1021/jp203915q |J. Phys. Chem. A 2011, 115, 9004–9013

Scheme 3

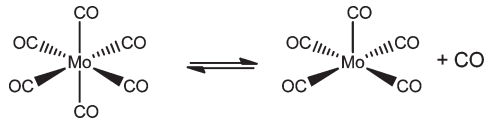

replaces a weaker bond. The variations in reaction volume are attributed to differences in bond length and in structural features that create excluded volumes.

Bond Energies. Using ΔH_{1avg} and the experimentally derived $Mo(CO)_5$—CO bond energy of 40.5 kcal mol^{-1} yields a $Mo(CO)_5$—alkane bond energy of 12.5 kcal mol^{-1}.[50,51] This bond energy should be an upper limit of the activation enthalpy for displacement of alkane by a Lewis base. For example, the activation enthalpy ($\Delta H_2^{\ddagger}$) for toluene displacement of cyclohexane on $Mo(CO)_5$—cyclohexane has been reported to be 8 kcal mol^{-1}.[48a] The displacement is proposed to occur via an interchange mechanism ($\Delta S^{\ddagger}$ = −7.6 cal mol^{-1} K^{-1}), and the activation enthalpy is expected to be less than the bond energy because there is residual metal—alkane bonding in the transition state. Likewise, $\Delta H_2^{\ddagger}$ was 7.8 kcal mol^{-1} for the interchange displacement of cyclohexane by CO ($\Delta S^{\ddagger}$ = −1.7 cal mol^{-1} K^{-1}).[48b] An even lower activation enthalpy (5 kcal mol^{-1}) was observed for the interchange displacement of heptane by CO in $Mo(CO)_5$—heptane ($\Delta S^{\ddagger}$ = −9.8 cal mol^{-1} K^{-1}).[48c] Previous DFT calculations of 4 kcal mol^{-1} for $Mo(CO)_5$—ethane have been reported,[52] which are likely to be more than 3 kcal mol^{-1} lower than for $Mo(CO)_5$—heptane if the trend is similar to $W(CO)_5$—alkanes.[53]

Inspection of ϕ_2 and ΔH_2 reveals that the amplitude of the slow component of the signal is dependent on the structure of the Lewis base. However, 1-hexene, 1-hexyne, triethylsilane, and THF have the same enthalpy within experimental error. Given that 1-hexene and 1-hexyne both form π complexes, their bond energies would be expected to be similar.[54] Relatively weak bond energies are expected for THF and triethylsilane because an ether oxygen and a Si—H bond are poor electron donors. It is likely a coincidence that their bond energies with the $Mo(CO)_5$ are similar to those measured for 1-hexyne and 1-hexene. The bond with benzene is much weaker than with the alkene because the delocalized benzene electrons are less available for sharing with the metal. This result is consistent with the well-known "inert" character that benzene has toward Lewis acids when compared to the reactivity of alkenes. Steric effects may also contribute to the weaker bond with benzene (vide infra).

The Mo—L bond energies are calculated from the Mo—CO bond energy, ΔH_{1avg} and ΔH_2 ($BE_{M-L} = BE_{M-CO} - \Delta H_{1avg} - \Delta H_2$, Table 1).[55] The Mo—hexene bond energy of 27 kcal mol^{-1} may be compared with Mo—alkene bond energies of 11.4, 12.6, and 15.1 kcal mol^{-1} for C_2Cl_4, C_2HCl_3, and 1,1-$C_2H_2Cl_2$, respectively, reported in a previous PAC study.[56] The series suggests replacing one chlorine atom with hydrogen increases the bond energy by 2—3 kcal mol^{-1}. A stronger bond for Mo—hexene is consistent with the trend; however, the trend would predict that the Mo—hexene bond energy should be no greater than 21 kcal mol^{-1}. The replacement of a hydrogen atom by an alkyl group may also increase the bond energy further, but an additional 6 kcal mol^{-1} increase seems unlikely. Part of the discrepancy is due in part to the fact that the incorrect quantum yield was used to study the chloroethylenes and that the effect of reaction volumes was not included. For example, in the case of 1-hexene, we find that ignoring the contribution of reaction volume by using a single solvent determination leads to a 3 kcal mol^{-1} error (Table 1, $\Delta H_2 - \Delta H_{2H}$).[57] In another study, DFT computations were used to determine $Mo(CO)_5$—ethene and $Mo(CO)_5$—ethyne bond energies of 18.8 and 18.0 kcal mol^{-1}, but the authors noted that their values for analogous chromium and iron carbonyl complexes were also lower (4 and 7 kcal mol^{-1}, respectively) than experimental values.[10]

The Mo—benzene bond energy has been estimated from the activation enthalpy of 12.5 ± 0.5 kcal mol^{-1} for the displacement of benzene by 1-hexene.[58] The value is 4 kcal mol^{-1} less than that in Table 1. However, the small activation entropy (4.1 ± 0.2 eu) suggests that the Mo—benzene bond is not completely broken in the transition state; therefore, the activation enthalpy should be less than the bond energy.[59] We conclude that a bond energy of 16.5 kcal mol^{-1} is consistent with the magnitude of this activation enthalpy.

Kinetics. The rate constants for the substitution of heptane by all of the Lewis bases vary a little more than an order of magnitude (Table 3) and do not correlate simply with the $Mo(CO)_5$—L bond energies (Table 1). For example, the bond energies for THF and 1-hexyne are the same, but the rate constant for THF is 12 times faster. The rate constants are too slow to be diffusion controlled, and the rate determining step in every case cannot be simply the dissociation of solvent followed by rapid attack of $Mo(CO)_5$ by a Lewis base; otherwise, the rate constant would be controlled by diffusion and essentially independent of the Lewis base structure. An interchange mechanism for alkane displacement on $M(CO)_5$(alkane) (M = Mo, W) by a Lewis base has been previously proposed[48a,b,d,60] and explains a trend in rate constants that is determined largely by steric effects. The largest rate constants (Table 3) occur for substitution with THT and THF, where the bonding electrons are lone pairs that extend far from a single nucleus, thus, minimizing steric effects. Next is 1-hexyne, where the bonding electrons are in a π bond where the electron density does not extend from the carbon as far as it does for the lone pairs of the hetero atoms. As a result, the metal must approach closer for orbital overlap and therefore is subject to a greater steric effect in the transition state. A similar situation occurs for 1-hexene, except a minimum of six equiplanar atoms must approach the metal. This approach requires a large free volume to engage the metal center. Benzene is only slightly slower than 1-hexene because its volume demand is similar. Except in pentane, the rate constant for triethylsilane addition is greater than the rate constant for 1-hexene but less than the rate constant for 1-hexyne. There appears to be two countering effects: the triethylsilane bonding electrons are in a σ orbital where the electron density extends an even shorter distance from the SiH interatomic axis, and an even closer approach is required for overlap to occur, but there are no other atoms attached to the hydrogen, so this reduces the steric effect.

The irradiation of $Mo(CO)_6$ has been studied previously at room temperature in neat 1-hexyne, where the metal alkyl σ-complex can be observed before it rearranges in 86 ps to the π-complex.[46] The authors proposed that the rearrangement is an intermolecular process, that is, a functional group of a free 1-hexyne displaces the alkyl group. Assuming the second-order rate constant for hexane displacement by 1-hexyne (3.1×10^7 M^{-1} s^{-1}, Supporting Information) is similar to the intermolecular displacement of the alkyl group in neat 1-hexyne (8.8 M), this rate would yield a lifetime of 3.7 ns, 43 times slower than that reported for the

Scheme 4

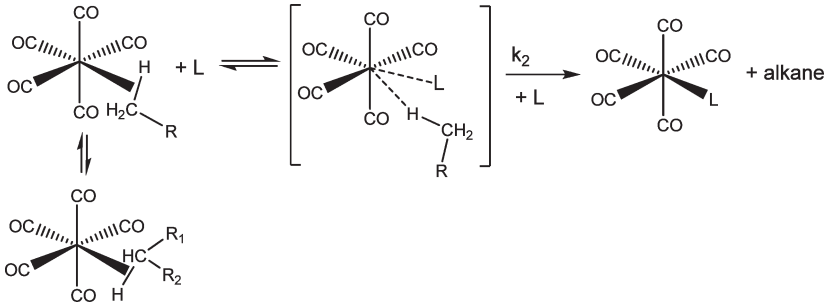

rearrangement. The lifetimes suggest another mechanism is operative for the rearrangement in neat 1-hexyne. An alternative mechanism was previously proposed for solvents having alkane chains with functional groups such as nitriles, alcohols, and alkyl bromides; the metal center walks along the chain without dissociation until it arrives at the functional group.[61,62]

Figure 5 reveals a decrease in the second-order rate constants for solvent displacement by the Lewis bases as the chain length increases. Viscosity is obviously dependent on chain length, and indeed, an inverse dependence on viscosity is observed for each ligand.[63] An inverse dependence is predicted by the von Smoluchowski−Stokes−Einstein equation, which relates diffusion rate constants to viscosity.[64] The current relationship appears to be coincidental since the rate constants and the activation energies reported in the literature are not consistent with a diffusion-controlled reaction (vide supra). The metal−solvent complex is anticipated to include a mixture of terminally and internally coordinated linear alkanes where displacement of a terminally coordinated linear alkane might be expected to be displaced more rapidly due to a lower steric hindrance (Scheme 4). We propose that the trend in Figure 5 can be attributed to the greater prevalence of internally coordinated linear alkane complexes as the chain length increases; thus, the rate of displacement decreases with increased chain length.[61]

Comparison of Computational and Experimental Results. The enthalpies of heptane displacement by various Lewis bases can be calculated from Tables 5−8 and are reported in Table 9 for comparison with PAC results. Although the precision is not high, the relative energies are in agreement. The error in the computational values is not well established for CO displacement, and higher level ab initio computations for these enthalpies are planned for improved calibration of these complexes. A major objective of this study was the computational determination of reaction volumes with enough accuracy that we could dispense with multisolvent studies. Obtaining single-solvent determinations of reaction enthalpies, corrected with computational volume calculations, would improve the efficiency of acquiring PAC measurements while significantly reducing experimental effort and cost. However, the comparisons and trends for reaction volumes are disappointing. There is no trend in the computational reaction volumes except that they are essentially all near zero. Because the estimated computational volume errors are so large, the results are within "experimental" volume errors of the PAC results, but the values are not precise enough for calculating "single point" enthalpies. It is clear from previous studies that reaction volumes cannot be assumed to be zero (vide supra). It should be noted that a good correlation is obtained between the computational molar volumes and experimental molar volumes (Figure 6) even though the absolute values are in poor agreement (Table 4). The slope of ~1.7 indicates that the computational values are systematically low. Therefore, the current approximations and assumptions involved in correlating the computational molar volume of an isolated gas phase molecule to a condensed phase experimental molar volume are insufficient. We suspect the major contribution to the error is the implicit assumption that the solvent is continuous. While the solvent "samples" all the space around the solute during collisions, the solvent does not fill this volume all the time as the solvent often is in transit. At any instant, there is an appreciable void volume not filled by the solvent. We are currently exploring alternative methods for calculating molecular and molar volumes. It is interesting that the correlation in Figure 6 is good considering that counterions were not included in the computational volumes for ions. Also, most of the experimental volumes in Table 4 were obtained using acetonitrile or water as the solvent, where electrostriction will be more important than in heptane. In fact, it has been previously noted that neutral compounds do give a slightly different (but experimentally significant) slope than that for ionic complexes.[44] Computational results for this correlation unfortunately do not significantly alter the calculated reaction volumes. Alternatively, reaction volumes might be best determined from partial molar volumes from high-precision density measurements. Unfortunately, this type of approach would be limited to compounds that have adequate solubility.

Table 9. Calculated Enthalpy and Volumes of Heptane Displacement by Lewis Base

	ΔH_2 (kcal mol^{-1})		ΔV_2 (mL mol^{-1})	
compound	computed	PAC	calculated	PAC
CO	−32.3	−28.0[a]	1.14	−14.4[a]
THF	−14.22	−13.8	2.05	−0.9
benzene	−6.02	−4.0	2.74	3.6
THT	−20.13	−23.6	0.68	−16
triethylsilane	−10.62	−13.8	1.79	−11.4
1-hexene	−17.31	−14.4	2.39	−9.0
1-hexyne	−16.03	−14.0	1.39	−2.0

[a] ΔH_2 and ΔV_2 for CO displacement of heptane are equal to $-\Delta H_1$ and $-\Delta V_1$, respectively.

dx.doi.org/10.1021/jp203915q | J. Phys. Chem. A 2011, 115, 9004–9013

CONCLUSIONS

Enthalpies of Lewis base addition determined by photoacoustic calorimetry and computational methods were in agreement and indicate relative metal ligand bond energies: CO > THT > 1-hexyne, 1- hexene, THF, triethylsilane > benzene. In contrast, the reaction volumes had a high degree of uncertainty and the results are inconclusive. Clearly, the contribution of the experimental reaction volume cannot be excluded; otherwise, the enthalpy results have errors as high as 4 kcal mol^{-1}. The rate constants of linear alkane solvent displacement by all of the Lewis bases were less than diffusion controlled and had a small but significant dependence on the length of the alkane chain. The dependence is attributed to differences in equilibria between terminally and internally coordinated linear alkanes.

ASSOCIATED CONTENT

Supporting Information. Schematic of PAC; values for ϕ_1, ϕ_2, and k in pentane, hexane, heptane, octane, decane, and dodecane for hexyne, hexene, triethylsilane, and benzene; additional computational data; and structures of ligands. This material is available free of charge via the Internet at http://pubs.acs.org.

AUTHOR INFORMATION

Corresponding Author

*Tel.: 901-678-2634. Fax: 901-678-3447. E-mail: tburkey@memphis.edu.

ACKNOWLEDGMENT

This work was partly supported by the National Science Foundation under Grant No. CHE-0911528 (T.J.B. and C.E.W). Quantum Northwest software was generously donated by Enoch Small.

REFERENCES

(1) To, T. T.; Heilweil, E. J.; Ruddick, K. R.; Webster, C. E.; Duke, C. B., III; Burkey, T. J. *J. Phys. Chem. A* **2009**, *113*, 2666–2676.

(2) (a) Nayak, S. K.; Farrell, G. J.; Burkey, T. J. *Inorg. Chem.* **1994**, *33*, 2236–2242. (b) Nayak, S. K.; Burkey, T. J. *J. Am. Chem. Soc.* **1993**, *115*, 6391–6397. (c) To, T. T.; Barnes, C. E.; Burkey, T. J. *Organometallics* **2004**, *23*, 2708–2714. (d) To, T. T.; Heilweil, E. J.; Burkey, T. J. *J. Phys. Chem A* **2006**, *110*, 10669–10673. (e) To, T. T.; Duke, C. B., III; Junker, C. S.; O'Brien, C.; Ross, C. R., II; Barnes, C. E.; Webster, C. E.; Burkey, T. J. *Organometallics* **2008**, *27*, 289–298. (f) Giordano, P. J.; Wrighton, M. S. *Inorg. Chem.* **1977**, *16*, 160–166. (g) Sorensen, A. A.; Yang, G. K. *J. Am. Chem. Soc.* **1991**, *113*, 7061–7063. (h) Brinkley, C. G.; Dewan, J. C.; Wrighton, M. S. *Inorg. Chim. Acta* **1986**, *121*, 119–125. (i) Wrighton, M. *Inorg. Chem.* **1974**, *13*, 905–909. (j) Pope, K. R.; Wrighton, M. S. *Inorg. Chem.* **1985**, *24*, 2792–2796. (k) Treichel, P. M.; Mueh, H. J. *Inorg. Chim. Acta* **1977**, *22*, 265–268.

(3) http://webbook.nist.gov/chemistry/om/

(4) (a) Bengali, A. A. *J. Organomet. Chem.* **2005**, *690*, 4989–4992. (b) Swennenhuis, B. H. G.; Benjamin, C., G.; Brothers, E. N.; Bengali, A. A. *J. Organomet. Chem.* **2010**, *695*, 891–897. (c) Kayran, C.; Richards, M.; Ford, P. C. *Inorg. Chim. Acta* **2004**, *357*, 143−148.

(5) Jiao, T.-J.; Leu, G.-L.; Farrell, G. J.; Burkey, T. J. *J. Am. Chem. Soc.* **2001**, *123*, 4960–4965. At room temperature, a change in the reaction volume of 3 mL mol^{-1} in heptane would give rise to an error of approximately 1 kcal mol^{-1} in the PAC-derived enthalpy.

(6) (a) King, J. C.; Zhang, J. Z.; Schwartz, B. J.; Harris, C. B. *J. Chem. Phys.* **1993**, *99*, 7595–7601. (b) Yu, S.-C.; Xu, X.; Lingle, R., Jr.; Hopkins, J. B. *J. Am. Chem. Soc.* **1990**, *112*, 3668–3669. (c) Lee, M.; Harris, C. B. *J. Am. Chem. Soc.* **1989**, *111*, 8963−8965. (d) Joly, A. G.; Nelson, K. A. *Chem. Phys.* **1991**, *152*, 69–82. (e) Simon, J. D.; Xie, X. *J. Phys. Chem.* **1989**, *93*, 291–293. (f) Joly, A. G.; Nelson, K. A. *Chem. Phys.* **1991**, *152*, 69–82. (g) Joly, A. G.; Nelson, K. A. *J. Phys. Chem.* **1989**, *93*, 2876–2878. (h) Simon, J. D.; Xie, X. *J. Phys. Chem.* **1987**, *91*, 5538–5540. (i) Simon, J. D.; Xie, X. *J. Phys. Chem.* **1986**, *90*, 6751–6753. (j) Wang, L.; Zhu, X.; Spears, K. G. *J. Am. Chem. Soc.* **1988**, *110*, 8695–8696.

(7) (a) Dougherty, T. P.; Heilweil, E. J. *Chem. Phys. Lett.* **1994**, *227*, 19–24. (b) Joly, A. G.; Nelson, K. A. *Chem. Phys.* **1991**, *152*, 69–82.

(8) (a) Dobson, G. R. *Acc. Chem. Res.* **1976**, *9*, 300–306. (b) Howell, J. A. S.; Burkinshaw, P. M. *Chem. Rev.* **1983**, *83*, 557–599.

(9) Brown, C. E.; Ishikawa, Y.-I.; Hackett, P. A.; Rayner, D. M. *J. Am. Chem. Soc.* **1990**, *112*, 2530–2536.

(10) Nechaev, M. S.; Rayon, V. M.; Frenking, G. *J. Phys. Chem. A* **2004**, *108*, 3134–3142.

(11) Bernstein, M.; Simon, J. D.; Peters, K. S. *Chem. Phys. Lett.* **1983**, *100*, 241–244. (b) Dobson, G. R.; Cate, C. D.; Cate, C. W.; Asali, K. *J. Inorg. Chem.* **1991**, *30*, 4471–4474.

(12) For leading references, see Gittermann, S.; Jiao, T.; Burkey, T. J. *Photochem. Photobiol. Sci.* **2003**, *2*, 817–820.

(13) Maciejewski, A.; Jaworska-Ausustyniak, A.; Szeluga, Z.; Wojtczak, J.; Karolczak, J. *Chem. Phys. Lett.* **1988**, *153*, 227–232.

(14) Braslavsky, S. E.; Heibel, G. H. *Chem. Rev.* **1992**, *92*, 1381–1410.

(15) Rudzki, J. E.; Goodman, J. L.; Peters, K. S. *J. Am. Chem. Soc.* **1985**, *107*, 7849–7854.

(16) Rudzki, J.; Libertini, L. J.; Small, E. W. *Biophys. Chem.* **1992**, *42*, 29–48.

(17) Ferrocene heat deposition.

(18) A quantum yield of 0.90 ± 0.02 for the photosubstitution of molybdenum hexacarbonyl in linear alkanes has been reported previously: see ref 19.

(19) Jiao, T.; Leu, G.-L.; Farrell, G. J.; Burkey, T. J. *J. Am. Chem. Soc.* **2001**, *123*, 4960–4965.

(20) Frisch, M. J.; Trucks, G. W.; Schlegel, H. B.; Scuseria, G. E.; Robb, M. A.; Cheeseman, J. R.; Scalmani, G.; Barone, V.; Mennucci, B.; Petersson, G. A.; Nakatsuji, H.; Caricato, M.; Li, X.; Hratchian, H. P.; Izmaylov, A. F.; Bloino, J.; Zheng, G.; Sonnenberg, J. L.; Hada, M.; Ehara, M.; Toyota, K.; Fukuda, R.; Hasegawa, J.; Ishida, M.; Nakajima, T.; Honda, Y.; Kitao, O.; Nakai, H.; Vreven, T.; Montgomery, Jr., J. A.; Peralta, J. E.; Ogliaro, F.; Bearpark, M.; Heyd, J. J.; Brothers, E.; Kudin, K. N.; Staroverov, V. N.; Kobayashi, R.; Normand, J.; Raghavachari, K.; Rendell, A.; Burant, J. C.; Iyengar, S. S.; Tomasi, J.; Cossi, M.; Rega, N.; Millam, N. J.; Klene, M.; Knox, J. E.; Cross, J. B.; Bakken, V.; Adamo, C.; Jaramillo, J.; Gomperts, R.; Stratmann, R. E.; Yazyev, O.; Austin, A. J.; Cammi, R.; Pomelli, C.; Ochterski, J. W.; Martin, R. L.; Morokuma, K.; Zakrzewski, V. G.; Voth, G. A.; Salvador, P.; Dannenberg, J. J.; Dapprich, S.; Daniels, A. D.; Farkas, Ö.; Foresman, J. B.; Ortiz, J. V.; Cioslowski, J.; Fox, D. J. *Gaussian 09*, Revision A.02; Gaussian, Inc.: Wallingford, CT, 2009.

(21) Becke, A. D. *Phys. Rev. A* **1988**, *38*, 3098–3100.

(22) (a) Perdew, J. P. *Phys. Rev. B* **1986**, *33*, 8822–8824. (b) Perdew, J. P.; Zunger, A. *Phys. Rev. B* **1981**, *23*, 5048–5079.

(23) Parr, R. G.; Yang, W. *Density Functional Theory of Atoms and Molecules*; Oxford University Press: New York, 1989.

(24) (a) Hay, P. J.; Wadt, W. R. *J. Chem. Phys.* **1985**, *82*, 299–310. (b) Wadt, W. R.; Hay, P. J. *J. Chem. Phys.* **1985**, *82*, 284–298.

(25) Couty, M.; Hall, M. B. *J. Comput. Chem.* **1996**, *17*, 1359–1370.

(26) Hariharan, P. C.; Pople, J. A. *Theor. Chim Acta* **1973**, *28*, 213–222. The 6-31G(d′) basis set has the d polarization functions for C, N, and O taken from the 6-311G basis set, instead of the original arbitrarily assigned value of 0.8 used in the 6-31G(d) basis set. Foresman, J. B.; Frisch, Æ. *Exploring Chemistry with Electronic Structure Methods*, 2nd ed.; Gaussian, Inc: Pittsburgh, PA, 1996, p 110.

(27) Francl, M. M.; Pietro, W. J.; Hehre, W. J.; Binkley, J. S.; DeFrees, D. J.; Pople, J. A.; Gordon, M. S. *J. Chem. Phys.* **1982**, *77*, 3654–3665.

(28) (a) Dunlap, B. I.; Connolly, J. W. D.; Sabin, J. R. *J. Chem. Phys.* **1979**, *71*, 3396–3402. (b) Dunlap, B. I.; Connolly, J. W. D.; Sabin, J. R.

J. Chem. Phys. **1979**, *71*, 4993–4999. (c) Dunlap, B. I. *J. Chem. Phys.* **1983**, *78*, 3140–3142. (d) Dunlap, B. I. *J. Mol. Struct. (THEOCHEM)* **2000**, *529*, 37–40.

(29) Webster, C. E.; Drago, R. S.; Zerner, M. C. *J. Am. Chem. Soc.* **1998**, *120*, 5509–5516.

(30) Webster, C. E.; Drago, R. S.; Zerner, M. C. *J. Phys. Chem. B* **1999**, *103*, 1242–1249.

(31) Zerner, M. C.; Ridley, J. E.; Bacon, A. D.; Edwards, W. D.; Head, J. D.; McKelvey, J.; Culberson, J. C.; Knappe, P.; Cory, M. G.; Weiner, B.; Baker, J. D.; Parkinson, W. A.; Kannis, D.; Yu, J.; Rösch, N.; Kotzian, M.; Tamm, T.; Karelson, M. M.; Zheng, X.; Pearl, G. M.; Broo, A.; Albert, K.; Cullen, J. M.; Cramer, C. J.; Truhlar, D. G.; Li, J.; Hawkins, G. D.; Liotard, D. A. *ZINDO*, a semiempirical program package; University of Florida: Gainsesville, FL, 1998.

(32) Pascual-Ahuir; J. L.; Silla, E.; Tunon, I. *QCPE*, Quantum Chemistry Program Exchange, Bloomington, Indiana; Program No. 554; 1988, 1992, 1994. http://www.ccl.net/ccl/qcpe/QCPE_removed/

(33) Pascual-Ahuir, J. -L.; Silla, E.; Tuñon, I. *J. Comput. Chem.* **1994**, *15*, 1127–1138.

(34) Silla, E.; Tunon, I.; Pascual-Ahuir, J.-L. *J. Comput. Chem.* **1991**, *12*, 1077–1088.

(35) The print control of the output file was set to verbose debug output [with the keyword IOP(3/33=9)]. The molecular volume from the second set of data of "GePol: Cavity volume" within the Gaussian output file was used to calculate the molar volume. This second set of data uses a smaller number of vertices to generate the tesserae which defines the molecular surface. All other default parameters were used.

(36) Bondi, A. *J. Phys. Chem. B* **1964**, *68*, 441–451.

(37) This situation holds true until the concentration of Lewis base is high enough that reactions are fast enough to contribute to ϕ_1. This concentration depends on the structure of the Lewis base and the transducer response time.

(38) At lower concentrations, ϕ_2 decreases to zero where the reaction with Lewis base becomes too slow to detect. At high concentration, ϕ_2 also decreases to zero as the reaction is so fast that it contributes to ϕ_1 not ϕ_2.

(39) The calculations neglect PV work done by volume change with respect to the barometric or P_i (internal pressure). For example, hexyne results for P_i = 0.0548 kcal/mL in alkane solvents:[40] ΔH_1 = 25.8 kcal/mol; ΔH_2 = −14.0 kcal/mol; ΔV_1 = 13.2 mL/mol; ΔV_2 = −2.23 mL/mol.

(40) Dack, M. R. J. *J. Chem. Educ.* **1974**, *51*, 231–234.

(41) An outlier is included on the plot as an ×. Although including the outlier makes a large change in the intercept (−10.1 ± 8.5 vs 1.8 ± 5.3 mL/mol), the errors are so large that it is not statistically significant. In contrast, the slope (−9.6 ± 2.5 vs −12.6 ± 1.5 kcal/mol) is less sensitive to the outlier.

(42) If the intercept is not constrained to zero, the slope is 1.792 (0.024), with an intercept of −23.6 (6.5) mL/mol.

(43) A computed molecular volume of 104.97 Å^3 molecule^{-1} is converted to a computed molar volume by multiplying by (1.0 × 10^{-8} cm)^3 Å^{-3} and Avogadro's number, which yields an uncorrected computed molar volume equal to 63.21 mL mol^{-1}.

(44) Tran, D.; Hunt, J. P.; Wherland, S. *Inorg. Chem.* **1992**, *31*, 2460–2464.

(45) (a) Lian, T. Q.; Bromberg, S. E.; Asplund, M. C.; Yang, H.; Harris, C. B. *J. Phys. Chem.* **1996**, *100*, 11994–12001. (b) Patterson, M. J.; Hunt, P. A.; Robb, M. A.; Takahasi, O. *J. Phys. Chem. A* **2002**, *102*, 10494–49504. (c) Trushin, S. A.; Fuss, W.; Schmid, W. E. *Chem. Phys.* **2000**, *259*, 313–330.

(46) Shanoski, J. E.; Payne, C. K.; Kling, M. F.; Glascoe, E. A.; Harris, C. B. *Organometallics* **2005**, *24*, 1852–1859.

(47) (a) Schwartz, B. J.; King, J. C.; Zhang, J. Z.; Harris, C. B. *Chem. Phys. Lett.* **1993**, *203*, 503–508. (b) Lian, T.; Bromberg, S. E.; Asplund, M. C.; Yang, H.; Harris, C. B. *J. Phys. Chem.* **1996**, *100*, 11994–12001.

(48) Rates of IR and UV−vis studies: (a) Diz, E. L.; Ford, P. C. *Inorg. Chim. Acta* **2008**, *361*, 3084–3088. (b) Kayran, C.; Richards, M.; Ford, P. C. *Inorg. Chim. Acta* **2004**, *357*, 143–148. (c) Breheny, C. J.; Kelly, J. M.; Long, C.; O'Keeffe, S.; Pryce, M. T.; Russell, G.; Walsh, M. M. *Organometallics* **1998**, *17*, 3690–3695. (d) Zhang, S.; Zang, V.; Bajaj, H. C.; Dobson, G. R.; van Eldik, R. J. *J. Organomet. Chem.* **1990**, *397*, 279–289.

(49) Schmidt, R.; Schütz, M. *Chem. Phys. Lett.* **1996**, *263*, 795–802.

(50) Lewis, K. E.; Golden, D. M.; Smith, G. P. *J. Am. Chem. Soc.* **1984**, *106*, 3905–3912.

(51) A selection of experimental values for the Mo−CO bond energy has been discussed in ref 19.

(52) Da Silva, J. C. S.; De Almeida, W. B.; Rocha, W. R. *Chem. Phys.* **2009**, *365*, 85–93.

(53) Brown, C. E.; Ishikawa, Y.-I.; Hackett, P. A.; Rayner, D. M. *J. Am. Chem. Soc.* **1990**, *112*, 2530–2536.

(54) There is the possibility that the 1-hexene and 1-hexyne π complexes could rearrange to an alkylidene or vinylidene, respectively. At least in the case of 1-hexyne, the rearrangement is known to be too slow to be observed in our PAC experiments (see ref 46 for a discussion of the rearrangement of 1-hexene and 1-hexyne π complexes).

(55) Equivalently, the Mo−CO bond energy can be calculated from the Mo−alkane bond energy and ΔH_2 because the Mo−alkane bond energy is calculated by using the Mo−CO bond energy.

(56) Schlappi, D. N.; Cedeño, D. L. *J. Phys. Chem. A* **2009**, *113*, 9692–9699.

(57) The authors used a quantum yield of 0.70 based on an assumed value in the literature. Using the correct quantum yield of 0.9, results in value 1 kcal mol^{-1} more exothermic. An additional error of 3 kcal mol^{-1} for neglect of reaction volume plus the 21 kcal mol^{-1} estimated in the text would yield 25 kcal mol^{-1} for the Mo−hexene bond energy. This is in much better agreement with the result for 1-hexene in Table 1.

(58) Zhang, S.; Dobson, G. R. *Inorg. Chim. Acta* **1991**, *181*, 103–109.

(59) It is a requirement that the activation free energy be a maximum at the transition state and not the activation enthalpy.

(60) Biber, L.; Reuvenov, D.; Revzin, T.; Sinai, T.; Zahavi, A.; Schultz, R. H. *Dalton Trans.* **2007**, 41–51.

(61) (a) Xie, X.; Simon, J. D. *J. Am. Chem. Soc.* **1990**, *112*, 1130–1136. (b) O'Driscoll, E.; Simon, J. D. *J. Am. Chem. Soc.* **1990**, *112*, 6580–6584.

(62) For other studies of rearrangement, see King, J. C.; Zhang, J. Z.; Schwartz, B. J.; Harris, C. B. *J. Chem. Phys.* **1993**, *99*, 7595–7601.

(63) See Supporting Information.

(64) Fischer, H.; Schuh, H. *Helv. Chim. Acta* **1978**, *61*, 2130–2164.